Chemical Physics Letters 531 (2012) 173–176

Contents lists available at SciVerse ScienceDirect

Chemical Physics Letters

journal homepage: www.elsevier.com/locate/cplett

Study of singlet excited state absorption spectrum of lutetium bisphthalocyanine using the femtosecond Z-scan technique

Marcelo G. Vivas [a,*], Edson G.R. Fernandes [a], María Luz Rodríguez-Méndez [b], Cleber R. Mendonca [b]

[a] Instituto de Física de São Carlos, Universidade de São Paulo, São Carlos, SP, Brazil
[b] Department of Inorganic Chemistry, Escuela de Ingenierías Industriales, University of Valladolid, 47011 Valladolid, Spain

ARTICLE INFO

Article history:
Received 6 December 2011
In final form 9 February 2012
Available online 21 February 2012

ABSTRACT

In this study we investigate the singlet excited state absorption of lutetium bisphthalocyanine ($LuPc_2$) over a wide spectral range. It was observed distinct nonlinear absorption behaviors; saturable (SA) and reverse saturable absorption (RSA). The RSA effect was observed below 640 and above 680 nm, while SA occurs around the Q-band region, located around 660 nm. To describe the main singlet–singlet transitions, we employed the rate equation model considering the simplified three-energy level diagram. Our results reveal a ratio between excited and ground state absorption smaller than 0.05 at the Q-band region, and of approximately 4 for the other regions.

1. Introduction

Metallophthalocyanines (MPs) have attracted great attention for technological applications because of their interesting optical and electrical properties, as well as high thermal, chemical and photochemical stability. Such compounds are π-conjugated macrocyclic molecules with a metal atom coordinated to the center [1]. This class of organic molecule has been applied for a wide range of systems, including photovoltaic material in solar cells [2], molecular electronics [3,4], sensors [3,4], electrochromic systems [5] and photodynamic therapy [6]. In optics, metallophthalocyanines are interesting candidates for applications because of their attractive nonlinear optical (NLO) properties, such as nonlinear refraction, excited state and two-photon absorptions [1,7,8]. Such properties may play significant role in several photonic devices, such as, for instance, optical switcher and optical power limiters [1,9]. The optical nonlinearity exhibited by MPs is related to some of their distinct structural features; (i) two-dimensionality of the π-conjugated system, (ii) modification of the electronic distribution of the macrocycle ring by the central metal, and (iii) the peripheral substituent groups [10].

Several types of MPs have been synthesized and studied by several groups. Among them, lanthanide bisphthalocyanines have been receiving considerable attention because of their rich electrochemical and electrochromic properties [11–13]. Since bisphthalocyanine are built of two phthalocyanine rings coordinated to a central metal ion, they can present enhanced optical nonlinearities due to the increasing of conjugation length and the interaction between macrocyclic rings and the lanthanide atom [14–16]. Therefore, lanthanide bisphthalocyanine has been proposed to be used in optical switching, optical recording, optical rectifying, optical limiting, frequency mixing, harmonic generation, etc. [17]. In the last few years, the nonlinear optical properties of the lutetium bisphthalocyanines ($LuPc_2$) have been studied using nanosecond and picosecond pulses [17–20]. Nevertheless, the use of such long duration laser pulses usually mixes up singlet and triplet states absorption in the optical nonlinearity. Moreover, most of the studies reported were performed only in a few wavelengths. Envisioning possible application of $LuPc_2$ in optoelectronic and photonic devices, in this Letter we study the NLO properties of $LuPc_2$ using 120-fs laser pulses with a 1 kHz repetition rate, over a wide spectral range. By using such pulses we were able to study the contribution exclusively from the singlet states to the nonlinear absorption process (excited state absorption).

2. Experimental

All chemicals were of reagent grade and used as supplied (Sigma–Aldrich). The neutral radical state $LuPc_2$ was synthesized and purified as described previously [21]. The $LuPc_2$ molecular structure is illustrated in Figure 1. We prepared $LuPc_2$/chloroform solutions with concentrations of 1.5×10^{-6} and 1.0×10^{-4} mol L^{-1}, for linear and nonlinear optical measurements, respectively. For the optical measurements the samples were placed in 2-mm thick fused silica cuvettes. The linear absorption spectrum was recorded using a Cary 17 UV–Vis–NIR spectrophotometer.

Excited state absorption measurements were carried out employing the open aperture Z-scan [22], using 120-fs laser pulses

* Corresponding author. Address: Instituto de Física de São Carlos – USP, P.O. Box 369, 13560-970 São Carlos, SP, Brazil. Fax: +55 16 3373 9811.
E-mail address: mavivas82@yahoo.com.br (M.G. Vivas).

0009-2614
doi:10.1016/j.cplett.2012.02.028

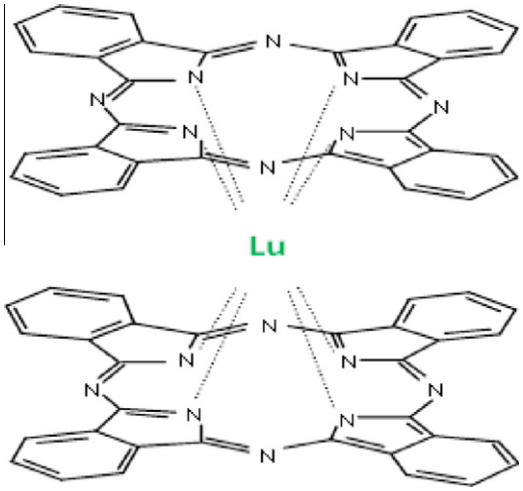

Figure 1. The molecular structure of the $LuPc_2$.

from an optical parametric amplifier pumped by 150-fs pulses at 775 nm, delivered by a Ti:sapphire chirped pulse amplified system, operating at 1-kHz repetition rate. The Z-scan measurements were carried out with energies ranging from 5 to 210 nJ/pulse, with beam waist size ranging from 14 to 21 μm. More details about the Z-scan setup employed are described in Ref. [23].

3. Results and discussion

The solid lines in Figure 2 represent the linear absorption spectrum of the $LuPc_2$ chloroform solution. The spectrum exhibits the two characteristic absorptions bands of $LuPc_2$, denominated B- and Q-band, located at 320 and 660 nm, respectively. Such bands are attributed to $\pi \rightarrow \pi^*$ transitions from the phthalocyanine ring, while the low-intensity absorption bands at 456 is related to $e_g \rightarrow a_{2u}$ electronic transition of Lu-phthalocyanine [12].

Figure 3 displays open aperture Z-scan signatures obtained at five distinct wavelengths in resonant conditions, i.e., in the linear absorption region of the $LuPc_2$. The increase in the normalized transmittance close to the focus ($Z = 0$) for wavelengths in the Q-band region (640–680 nm) indicates that the material's excited state absorption cross-section is smaller than the ground state one, characterizing a saturable absorption (SA) effect. On the other hand, the decrease observed in the normalized transmittance below 640 and above 680 nm indicates that for those regions the

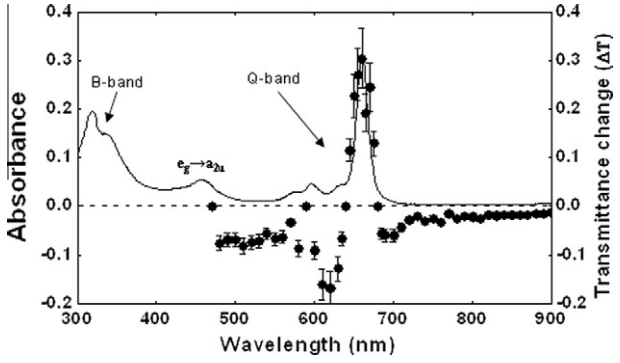

Figure 2. Linear absorption (solid line) and transmittance change (solid circles) spectra for $LuPc_2$. The results presented in the nonlinear spectrum were carried out with energies ranging from 5 to 150 nJ/pulse, with beam waist size ranging from 14 to 21 μm.

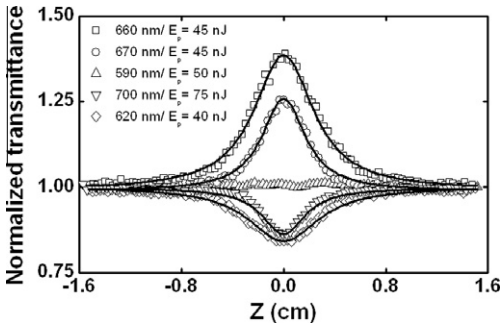

Figure 3. Open aperture Z-scan signature for $LuPc_2$/chloroform solution at 660 (squares), 670 (circles), 590 (triangles up), 700 nm (triangles down) and 620 (diamonds). The inset shows the pulse energy (E_p) used to obtain different Z-scan signatures. The concentration used to measure the SA effect was 5–10 times smaller than to RSA effects.

excited state absorption cross-section is higher than the one from the ground state, which characterizes a reverse saturable absorption (RSA). No changes in the normalized transmittance were observed at 640 nm (triangles) because at this spectral region the SA and RSA effects cancel each other, since in both cases, the ground and excited state absorption cross-section are practically the same. Such wavelengths demarcates the regions where the effects change from RSA to SA (640 nm) and from SA to RSA (680 nm).

The solid circles in Figure 2 represents the transmittance change (ΔT) obtained from the Z-scan curves (similar to the ones shown in Figure 3) as a function of the wavelength, from 470 up to 850 nm. The two distinct behaviors previously mentioned can clearly be observed in Figure 2 (solid circles); (i) a SA process that follows the Q-band peak (positive ΔT values), (ii) a RSA process below 640 and above 680 nm (negative ΔT value). We show in Figure 4 the transition from SA to RSA at 637 nm and RSA to SA at 677 nm that appears in the Z-scan curves. Such results indicate a competition between different effects that occurs for wavelength around the Q-band.

To interpret the transmittance change spectrum obtained for $LuPc_2$ (Figure 2 – solid circles), we used the excited states energy diagram obtained by Orti et al. employing Valence Effective Hamiltonian (VEH) calculations [24] (Figure 5a). According to this diagram, by tuning the excitation wavelength in the Q-band region, molecules at the a_{2u} level are promoted to e_g^* level ($a_{2u} \rightarrow e_g^*$ transition), being subsequently excited to a higher excited energy

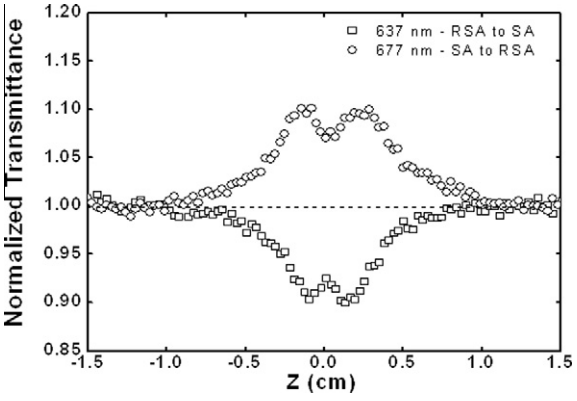

Figure 4. Open aperture Z-scan signature for $LuPc_2$/chloroform solution obtained at 637 nm (squares) and 677 nm (diamonds) using pulse energy of approximately 20 nJ. Such results indicate a competition between different effects that occurs for wavelength around the Q-band.

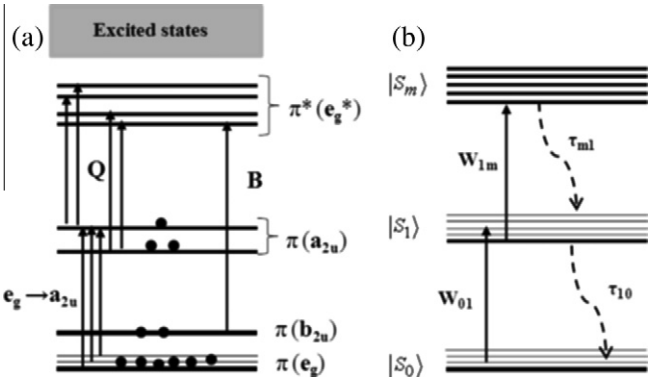

Figure 5. (a) Excited states diagram of the $LuPc_2$ obtained by Orti et al. using valence effective Hamiltonian calculations [24]. (b) Simplified three-energy-level diagram used to model the excited state cross-section spectrum within of the rate equation model.

level. Such excitation route can be conveniently described by the simplified three-energy-level diagram presented in Figure 5b, considering also the relaxation pathways from $|S_m\rangle \rightarrow |S_1\rangle$ (higher excited state to e_g^*, with a decay time τ_{m1}) and from $|S_1\rangle \rightarrow |S_0\rangle$ ($e_g^* \rightarrow a_{2u}$, with a characteristic time τ_{10}). When the pump is tuned at the $e_g \rightarrow a_{2u}$ transition region, molecules at the a_{2u} level are re-excited to a higher energy level ($|S_m\rangle$). Again, such excitation pathway can also be described by the same three-energy-level diagram presented in Figure 5b. In this case, however, molecules at a_{2u} level decay radiatively to the ground state with a characteristic relaxation time τ_{10} ($|S_1\rangle \rightarrow |S_0\rangle$). Therefore, at both excitation regions the transitions can be described by the three-energy-level diagram (Figure 5b). Thus, using this approach, the population of each state can be described by the following rate equations:

$$\frac{dn_0}{dt} = -w_{01}n_0 + \frac{n_1}{\tau_{10}}, \tag{1}$$

$$\frac{dn_1}{dt} = +w_{01}n_0 - w_{1m}n_1 - \frac{n_1}{\tau_{10}} + \frac{n_m}{\tau_{m1}}, \tag{2}$$

$$\frac{dn_m}{dt} = +w_{1m}n_1 - \frac{n_m}{\tau_{m1}}, \tag{3}$$

where n_i are the population fractions of the states ($i = 0, 1, m$) with $n_0 + n_1 + n_m = 1$. $w_{01} = \sigma_{01}I(t)/h\nu$ and $w_{1m} = \sigma_{1m}I(t)/h\nu$ are the one-photon transition rates, with σ_{01} and σ_{1m} being the ground and excited state absorption cross-sections, respectively. The set of differential equations (Eqs. (1)–(3)) are numerically solved considering a Gaussian temporal profile for the laser pulse. The temporal dependence of the absorption coefficient is given by:

$$\alpha(t) = N\{n_0(t)\sigma_{01} + n_1(t)\sigma_{1m}\}, \tag{4}$$

where N is the sample concentration in molecules/cm^3. The transmittance can be calculated by integrating the propagation equation, $dI/dz = -\alpha(t)I(t)$, over the sample thickness and the full pulse width (t from $-\infty$ to $+\infty$). The absorption coefficient, α_{01}, is obtained from the linear absorption spectrum and is directly related to the ground state absorption cross-section by $\sigma_{01} = \alpha_{01}/N$. In this model we used $\tau_{10} = 60$ ps for the first excited state lifetime. Such value was obtained from Ref. [18], in which the transient absorption spectra of $LuPc_2$ in dichloromethane was investigated from 450 to 800 nm. For the relaxation time between excited states ($|S_m\rangle \rightarrow |S_1\rangle$) we used a value in the order of tens to hundreds of femtoseconds, which is in good agreement with experimental results obtained by Rao and Rao [25] for similar molecules. Hence, by fitting the Z-scan data (as the ones presented in Figure 2) employing the rate equation model proposed we determine the excited state absorption cross-section (σ_{1m}), since the others parameters (σ_{01}, τ_{10}, τ_{m1}) are kept fixed during the calculation. In Figure 6 we show the ground (σ_{01} – solid line) and excited state (σ_{1m} – squares) absorption cross-section spectra for $LuPc_2$ in chloroform we obtained considering the three-energy-level modeling employed.

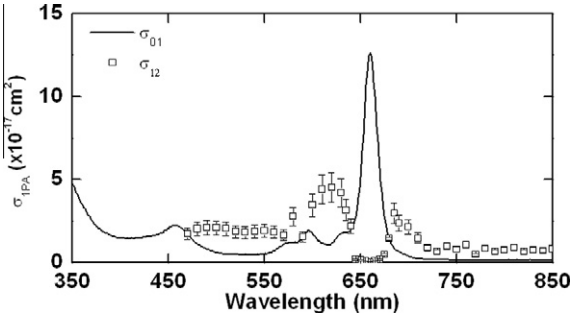

Figure 6. Ground (solid lines) and excited (empty squares) state absorption cross-section spectra for $LuPc_2$/chloroform solution obtained using the rate equation model.

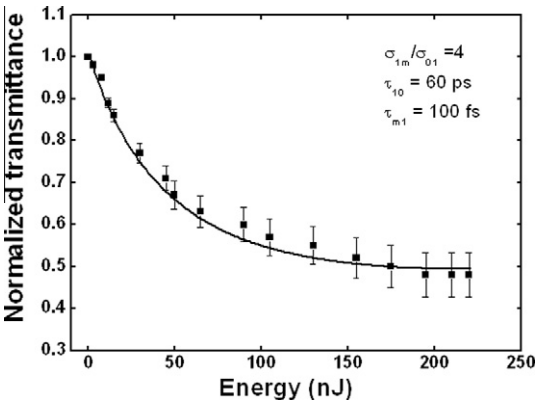

Figure 7. Transmittance as a function of incident energy at 530 nm. The solid lines represent the fit obtained using the simplified rate equation model.

It is observed that the excited state absorption spectrum (σ_{1m}) exhibits a strong SA process around the Q-band peak, with a cross-section ratio $\sigma_{1m}/\sigma_{01} < 0.05$. Such process is related to the population accumulated in the first excited state, since electronic transitions between excited states are practically neglected in this region. Moreover, the spectrum presents two regions with a considerable RSA process; one below 630 nm ($\sigma_{1m}/\sigma_{01} \sim 4.0$) and the other above 690 nm ($\sigma_{1m}/\sigma_{01} \sim 3.0$). Unlike other studies presented in the literature [18,19], due to the ultrashort pulses regime employed here, no triplet state is being populated and, therefore, only the singlet state contributes to the observed nonlinear optical process. Additionally, the magnitude of the excited state cross-sections determined here for $LuPc_2$ are similar to those obtained for ytterbium bisphthalocyanine [26] using the white-light continuum Z-scan technique.

In order to explore the potential of $LuPc_2$ to develop optical power limiting devices, in Figure 7 we display the normalized transmittance as a function of the incident energy at 530 nm, since in this wavelength we obtained RSA with a reasonable ratio between excited and ground state cross-section. As can be seen, the $LuPc_2$ presents an optical power limiting performance of approximately 50% for pulse energies higher than 150 nJ. The solid line corresponds to the fitting obtained using the rate equation model at 530 nm, from which we determined a ratio between

excited and ground state absorption cross-section of *ca.* 4. Such value is in good agreement with the one obtained at 532 nm with nanosecond and picosecond pulses [17,19].

4. Conclusion

The excited state absorption spectrum of the $LuPc_2$ was investigated, for the first time, employing the Z-scan technique with femtosecond pulses at a wide spectral range. Our results shown that the $LuPc_2$ dissolved in chloroform present distinct nonlinear absorption behaviors when excited by ultrashort pulses. Based on these results, we explained and determined the magnitude of the excited state absorption cross-section for the different processes using a simplified three-energy-level diagram. We observe a strong saturable absorption around the Q-band peak with the excited state absorption cross-section close to zero and a considerable reverse saturable absorption in two other regions (below 640 and above 690 nm). Moreover, we show that there are regions where the effects change from RSA to SA and vice versa, as well as regions in which there are a competition between them. These data complement other ones performed in a single wavelength (532 nm) reported in the literature using nanosecond and picosecond pulses, allowing a better understanding of the excited state dynamic in this type of metallophthalocyanine. In this context, the results shown here may contribute to the development of new photonic devices, such as saturable absorbers and optical power limiters.

Acknowledgments

Financial support from FAPESP (Fundação de Amparo à Pesquisa do estado de São Paulo), CNPq (Conselho Nacional de Desenvolvimento Científico e Tecnológico), Coordenação de Aperfeiçoamento de Pessoal de Nível Superior (CAPES) and MCINN (AGL 2009-12660/ALI).

References

[1] C.C. Leznoff, A.B.P. Lever, Phthalocyanines – Properties and Applications, VCH Publishers, New York, 1989.
[2] M.G. Walter, A.B. Rudine, C.C. Wamser, J. Porphyrins Phthalocyanines 14 (2010) 759.
[3] E.G.R. Fernandes, N.C.S. Vieira, A.A.A. de Queiroz, F.E.G. Guimaraes, V. Zucolotto, J. Phys. Chem. C 114 (2010) 6478.
[4] F.J. Pavinatto et al., J. Mater. Chem. 21 (2011) 4995.
[5] R.J. Mortimer, A.L. Dyer, J.R. Reynolds, Displays 27 (2006) 2.
[6] T. Lopez et al., Nanomed. Nanotechnol. Biol. Med. 6 (2010) 777.
[7] M. Drobizhev, N.S. Makarov, Y. Stepanenko, A. Rebane, J. Chem. Phys. 124 (2006) 224701.
[8] J.W. Perry, K. Mansour, S.R. Marder, K.J. Perry, D. Alvarez, I. Choong, Opt. Lett. 19 (1994) 625.
[9] M. Calvete, G.Y. Yang, M. Hanack, Synth. Met. 141 (2004) 231.
[10] B. Derkowska, M. Wojdyla, R. Czaplicki, W. Bala, B. Sahraoui, Opt. Commun. 274 (2007) 206.
[11] C. Bariain, I.R. Matias, C. Fernandez-Valdivielso, F.J. Arregui, M.L. Rodriguez-Mendez, J.A. de Saja, Sens. Actuators B – Chem. 93 (2003) 153.
[12] M.L. Rodriguez-Mendez, R. Aroca, J.A. Desaja, Chem. Mater. 4 (1992) 1017.
[13] R. Weiss, J. Fischer (Eds.), Lanthanide phthalocyanine complexes. Academic Press, New York, New York, 2003.
[14] M.J.F. Calvete, D. Dini, S.R. Flom, M. Hanack, R.G.S. Pong, J.S. Shirk, Eur. J. Org. Chem. (2005) 3499–3509.
[15] C.R. Mendonca, L. Gaffo, L. Misoguti, W.C. Moreira, O.N. Oliveira, S.C. Zilio, Chem. Phys. Lett. 323 (2000) 300.
[16] R. Rousseau, R. Aroca, M.L. Rodríguez-Méndez, J. Mol. Struct. 356 (1995) 49.
[17] L.C. Liu, C.H. Tai, A.T. Hu, T.H. Wei, J. Porphyrins Phthalocyanines 8 (2004) 984.
[18] A. Germain, T.W. Ebbesen, Chem. Phys. Lett. 199 (1992) 585.
[19] T.C. Wen, I.D. Lian, Synth. Met. 83 (1996) 111.
[20] C.R. Mendonca, L. Gaffo, W.C. Moreira, O.N. Oliveira, S.C. Zilio, Synth. Met. 121 (2001) 1477.
[21] Y. Gorbunova, M.L. Rodriguezmendez, J. Souto, L. Tomilova, J.A. Desaja, Chem. Mater. 7 (1995) 1443.
[22] M. Sheikbahae, A.A. Said, T.H. Wei, D.J. Hagan, E.W. Vanstryland, IEEE J. Quantum Electron. 26 (1990) 760.
[23] S.L. Oliveira, D.S. Correa, L. Misoguti, C.J.L. Constantino, R.F. Aroca, S.C. Zilio, C.R. Mendonca, Adv. Mater. 17 (2005) 1890.
[24] E. Orti, J.L. Bredas, C. Clarisse, J. Chem. Phys. 92 (1990) 1228.
[25] S.V. Rao, D.N. Rao, J. Porphyrins Phthalocyanines 6 (2002) 233.
[26] L. De Boni, L. Gaffo, L. Misoguti, C.R. Mendonca, Chem. Phys. Lett. 419 (2006) 417.